EPJ Web of Conferences **76**, 01023 (2014)
DOI: 10.1051/epjconf/20147601023

Conjugate heat transfer during viscous liquid movement in the open cavity, considering its cooling through outer boundary of back surface

A.V. Krainov[a] and G.V. Kuznetsov

Tomsk Polytechnic University, 634050 Tomsk, Russian

Abstract. Numerical simulation was carried out for nonisothermal incompressible viscous liquid in the open rectangular cavity, considering the heat loss through the channel bottom outer boundary. Liquid flow pattern and temperature profiles were obtained for solid and liquid phases. Influence of model parameters on heat carrier motion pattern and cavity cooling mode has been investigated.

The interest in studies of convective flow in different heat transfer conditions and for various cavities is caused by a wide applied value of the problem. Large amount of heating devices is being used in power plants and energy systems, production processes of a various complexity level. The necessity of studying these processes is determined by development of such energy-intensive indistries as power engineering, metallurgy, chemical industry and many other [1–5].

Experimental development of technologies always assumes a high probability of selecting not the best process conditions both for productivity and quality, and for implementation costs. Therefore, there arises a necessity to study theoretical hydrodynamic regularities and heat transfer during heat carrier motion in limited space.

This article considers nonsteady interaction of liquid with the open cavity (Fig. 1). Process of molten metal movement in the channel is being investigated with consideration to heat exchange with its walls. Thermal and physical characteristics of the molten metal and cavity walls are identical. The purpose of this work is to investigate the hydrodynamics and conjugate heat transfer during movement of nonisothermal incompressible viscous liquid in the rectangular-type cavity in conditions of the channel's outer boundary cooling. Similar problems have been solved before [6–8] for thermal insulation conditions of the cavity outer boundaries.

Study of the described process was done using a mathematical model based on the Navier-Stokes equations in the variables "vortex-stream function", the energy equation, and the heat-conduction equation for the cavity material with corresponding initial and boundary conditions

$$\frac{\partial \omega}{\partial \tau} + U\frac{\partial \omega}{\partial X} + V\frac{\partial \omega}{\partial Y} = \frac{1}{Re}\left(\frac{\partial^2 \omega}{\partial X^2} + \frac{\partial^2 \omega}{\partial Y^2}\right) \quad (1)$$

[a] Corresponding author: lux_veritatis@mail.ru

$$\frac{\partial^2\psi}{\partial X^2}+\frac{\partial^2\psi}{\partial Y^2}=\omega \tag{2}$$

$$\frac{\partial\theta}{\partial\tau}+U\frac{\partial\theta}{\partial X}+V\frac{\partial\theta}{\partial Y}=\frac{1}{Re\ \cdot \mathrm{Pr}}\left(\frac{\partial^2\theta}{\partial X^2}+\frac{\partial^2\theta}{\partial Y^2}\right) \tag{3}$$

$$\frac{\partial^2\theta_1}{\partial X^2}+\frac{\partial^2\theta_1}{\partial Y^2}=\frac{\partial\theta_1}{\partial \mathrm{Fo}}\cdot \tag{4}$$

System of Eqs. (1)–(4) was formulated by analogy with the problem formulations in transformed variables "ω-ψ" [9], applied for heat and mass transfer process simulation in conditions of free and mixed convection in the areas with local energy sources [10, 11] and intensive phase transformations in conditions of liquid fuel ignition [12, 13].

Numerical solution to the problem (1)–(4) is done in the area 2 (Fig. 1), limited by permeable boundaries (areas of entrance and exit from the cavity) and the inner (cavity side wall and bottom, and the jet symmetry line). Here Fo – Fourier number; Re – Reynolds number; Pr – Prandtl number; θ – dimensionless temperature of liquid; θ_1 – dimensionless temperature of cavity material; X, Y– dimensionless Cartesian coordinates; U, V – dimensionless transverse and cross velocity components of liquid motion, accordingly; ω, ψ – variables "vortex-stream function".

For the lower boundary ($y = S$, $D < x < L$) and side ($x = D$, $S < y < H$) the impermeability and adhesion conditions are specified, as well as boundary condition of the fourth kind for the energy equation (the problem is solved in conjugate formulation).

Conditions of heat-flux continuity and nonpenetration are specified on the symmetry axis ($x = L, S < y < H$). In the area of exit there were specified conditions of "drift" and "soft" boundary condition for velocity and temperature accordingly [9].

Thermal insulation conditions are specified for the outer boundaries, except for bottom area ($y = 0, 0 < x < L$), for which a boundary condition of the third kind is taken (intensive heat exchange with ambient medium is simulated):

$$\frac{\alpha\delta_y}{\lambda}\Delta\theta=-\frac{\partial\theta_1}{\partial Y}\cdot$$

The following notation is taken for boundary conditions in Fig. 1: x, y – dimensional horizontal and vertical Cartesian coordinates accordingly; L– linear dimension of cavity along the x-axis; H – linear dimension of cavity along the y-axis; D – linear dimension of cavity wall along the x-axis; S – linear dimension of cavity wall along the y-axis; $\Delta\theta$ – difference of dimensionless temperatures between outer boundary ($y = 0, 0 < x < L$) and ambient medium; α – heat-transfer coefficient; λ – heat conductivity; δ_y – wall thickness along the y-axis; u, v – dimensional transverse and cross components of liquid velocity accordingly; T^0, v^0 – initial dimensional values of temperature and velocity.

When formulating the problem, the following assumptions were made: 1) material of liquid and solid phases is identical; 2) thermal and physical parameters of liquid and wall material are taken identical; 3) laminar flow regime is realized; 4) possible effects of gas release, caused by chemical and physical processes, were not considered.

The Navier-Stokes equation system was solved in variables "vortex-stream function", the energy equation and heat conduction equation by the finite-difference method [9]. Difference analogs of transfer and heat conduction equations are solved using the sweep method [9]. The Poisson's equation for every sacrificial layer was solved using the successive over-relaxation method. Difference scheme of the second order accuracy was used.

Calculations were based on uniform and nonuniform difference grids. Evaluation of numerical simulation results validity was done by conservation check of the used difference scheme by a similar method, applied in [14, 15].

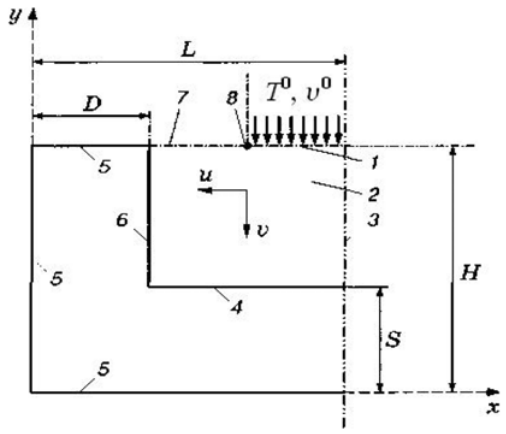

Figure 1. General diagram of flow in the cavity and geometry of computational domain (1–8): 1, 7 – permeable areas (areas of entrance and exit accordingly); 2 – hydrodynamic area; 3 – symmetry axis; 4,6 – inner surfaces; 5 – outer surfaces; 8 – boundary line between the permeable areas.

Liquid of a different type (water, molten lead, liquid steel, and fuel oil) was studied during the numerical survey with a wide variation range of the dynamic parameter Re and model parameters. This article presents the mathematical modeling of the described processes for liquid steel. In Figs. 2–4 the characteristic results of numerical surveys are given.

Based on the analysis of steady-state flow for different variants of cavity's geometric characteristics for a wide range of Reynolds numbers variation $40 \leq \mathrm{Re} \leq 1200$, two stages are specified. The first stage includes liquid movement from the area of entrance to the lower boundary of cavity. When liquid interacts with cavity bottom, the flow is slowing down and accompanied by the increased pressure, what leads to liquid steel spreading along the cavity bottom surface. In the second stage the liquid moves from cavity bottom to the exit area, forming the reverse flow area with recirculation zones. Liquid steel slowing continues in this sector, resulting in increased pressure area. Characteristic areas of forward and reverse flows, corresponding to the described stages of liquid movement in the channel, are given in Fig. 2.

Results analysis shows that distribution pattern of velocity cross component is maintained qualitatively during the first stage of movement. In the second stage occurs a change in the distribution pattern, caused both by reverse flow and its influence of dynamic parameters and geometric characteristics of cavity. The Reynolds numbers increase in conditions of heat removal via lower outer boundary (bottom), the profile of velocity cross component in initial cavity cross-sections becomes more filled and close to constant value. Two maximums of forward and reverse flows are formed, which start shifting (this is well seen from comparison of profiles under study in conditions of thermal insulation of the cavity's outer boundaries) along the X axis towards the side surface. When liquid moves towards the channel bed, the velocity cross component decreases in conditions of transverse component growth (Fig. 3). In the reverse stage of movement towards the exit area, the transverse component decreases, and function V in X starts increasing, what serves as a good demonstration of physical features of the process. From the Figs. 2, 3 it follows that the cross velocity decreases with the transverse component increasing in the area $0.27 < y < 0.36$, when liquid approaches the channel bed. The cross component starts growing in the reverse part of movement – the most intensive growth of this value is observed in the area $0.39 < y < 0.48$, $0.26 < x < 0.4$.

The impact on flow characteristics of the entrance region length (α) was also considered. Figure 4 shows the distribution of the cross component of velocity for various dimensions of the entrance region:

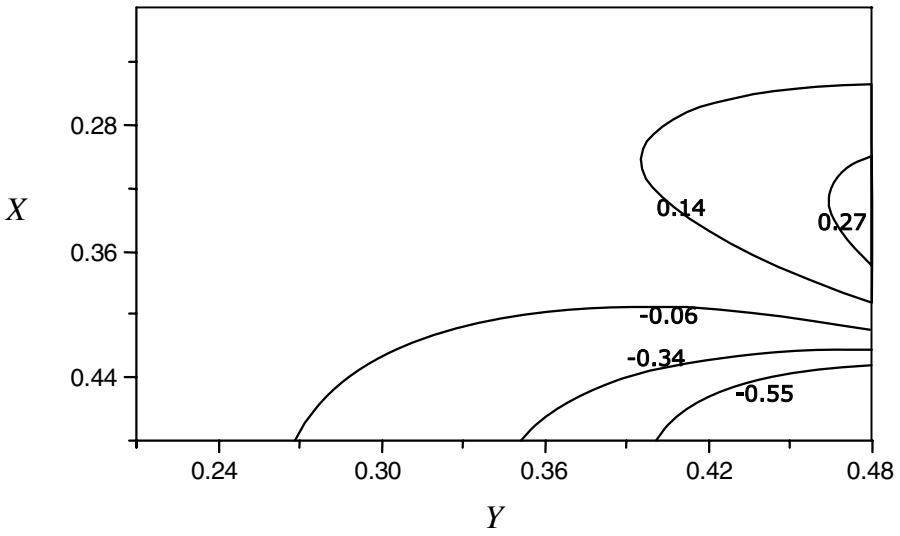

Figure 2. Isolines of velocity cross component at the time point $\mathrm{Fo} = 4.8 \cdot 10^{-2}$ with the number $\mathrm{Re} = 400$ and geometric ration of cavity sides $L/H = 1$.

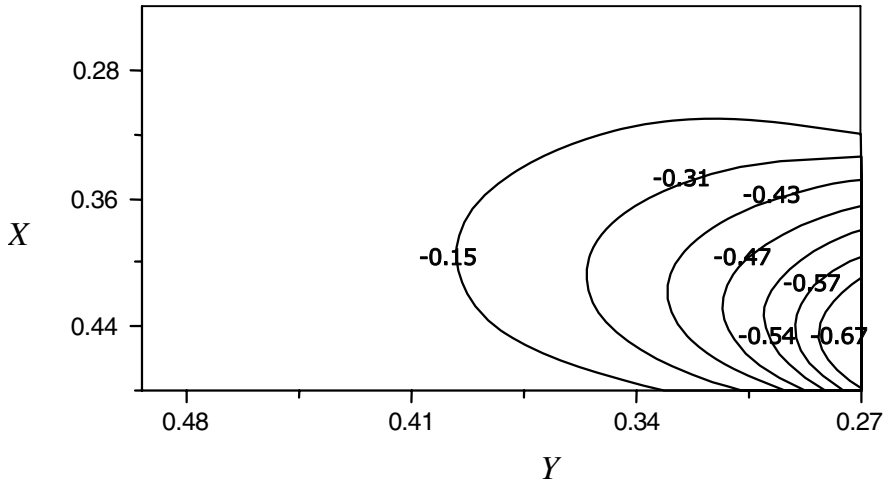

Figure 3. Isolines of the velocity transverse component at the time point $\mathrm{Fo} = 4.8 \cdot 10^{-2}$ with the number $\mathrm{Re} = 400$ and geometric ratio of cavity sides $L/H = 1$.

1) $\alpha = 0.2\alpha_*$ (solid lines); 2) $\alpha = 0.31\,\alpha_*$ (dashed). Here α_* – symbol of the full length of the cavity permeable region $y = H, D < x < L$. The given curves 1 and 2 correspond to the function $V(X)$ in the sections $Y = 0.745$ and $Y = 0.439$. With the increasing of the entrance region length, the maximum value of velocity cross component decreases slightly in the permeable areas of the cavity, it is especially well registered in the initial sections. Behavior of the function $V(X)$ is maintained qualitatively in various sections of the cavity with the entrance region length variation. Decrease of the entrance region length results in decrease of the maximum function value $U(X)$ in sections and in change of the distribution pattern.

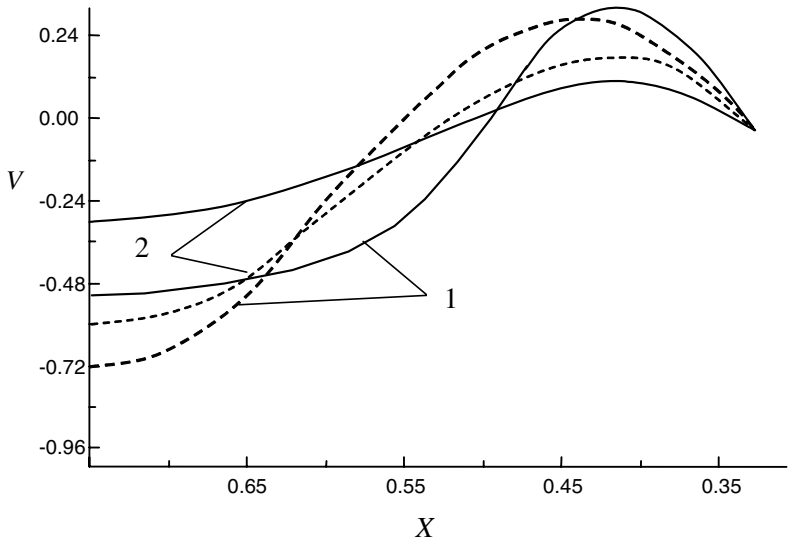

Figure 4. Distribution of velocity cross component for various dimensions of the area of liquid flowing in the cavity: 1) $\alpha = 0.2\,\alpha_*$ (solid lines); 2) $\alpha = 0.31\alpha_*$ (dashed lines). Curves 1 correspond to values of velocity cross component in the sections $Y = 0.745$; 2- $Y = 0.439$.

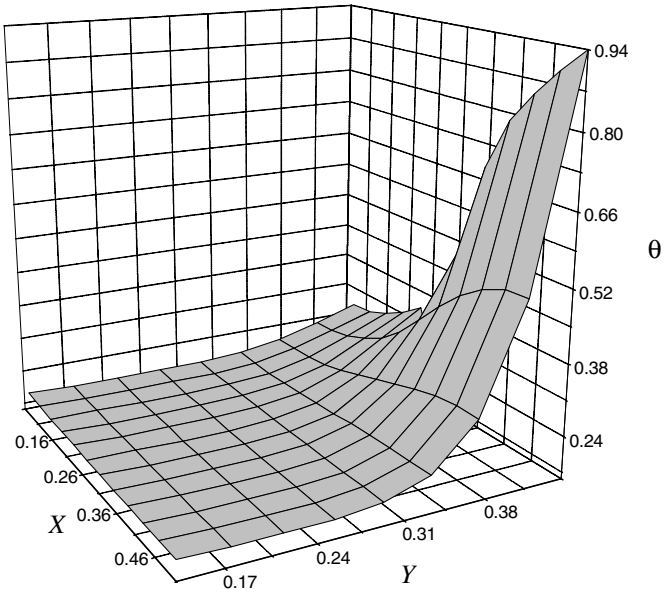

Figure 5. Temperature distribution in solid and liquid phases in the plane X, Y at the time moment $\mathrm{Fo} = 4,8 \cdot 10^{-2}$ with $\mathrm{Re} = 400$, $\mathrm{Pr} = 0.979$ and geometric ratio of the cavity sides $L/H = 1$.

Distribution of temperatures in solid and liquid phases are given in Fig. 5 in the plane X, Yat the time point $\mathrm{Fo} = 4,8 \cdot 10^{-2}$ with $\mathrm{Re} = 400$, $\mathrm{Pr} = 0.979$ and geometric ratio of cavity sides $L/H = 1$. The temperature distribution pattern in a liquid phase in the sections is much more obvious than in the solid one in conditions of heat removal through and outer lower surface of the cavity. Temperature

varies quite widely in the area $0.34 < y < 0.45, 0.31 < x < 0.5$. The hydrodynamic temperature profile becomes more full at $0.26 < y < 0.34, 0.27 < x < 0.5$. Based on the presented analysis, it follows that with the increase of the entrance region length the temperature profile changes more smoothly in cavity height, and the time of its inner surfaces filling decreases. In case of α value decrease, the temperature field changes more sharply in cavity height and the time of filling profile near the inner walls decreases.

Pattern of temperature distribution in liquid and solid phases is maintained qualitatively with variation of dynamic parameters, entrance region dimensions and geometric ratios. The range of temperature variation in the context of external heat transfer for the processes under study increases considerably, what provides a significant impact on liquid flow structure.

Numerical analysis results allow evaluating the impact of the cavity bottom outer surface cooling on heat transfer conditions and hydrodynamic profile of heat carrier flow.

The conducted studies allow for a conclusion about possibility of expanding the scope of mathematical tools [6–8] application for solving conjugate problems about convective flows in open cavities of a more complex geometry and heat transfer conditions in the outer boundaries.

References

[1] N.N. Rykalin, A.A. Uglov, L.M. Anischenko, High-Temperature production processes. Thermophysical basics (1985)
[2] G.V. Makhnova, V.V. Ris, E.M. Smirnov, Collection of the 2nd National Heat and Mass Transfer Conference **3**, 100 (1998)
[3] A.G. Fedorov, R. Viskanta, J. Heat Mass Transfer, 399 (2000)
[4] A.V. Krainov, Conjugate heat exchange for a viscous incompressible fluid moving in a rectangular cavity under conditions non-uniformity phase characteristics, Proceedings of International Conference Conjugate problems of mechanics, computer science and ecology, 302 (2004)
[5] G.V. Kuznetsov, M.A. Sheremet, J. Thermophysics and Aeromechanics **12**, 287 (2005)
[6] A.V. Krainov, J. Izvestiya TPU **306**, 84 (2003)
[7] G.V. Kuznetsov, A.V. Krainov, G.V. Shvalova, J. In the world of scientific discoveries **12**, 119 (2010)
[8] G.V. Kuznetsov, A.V. Krainov, J. Applied Mechanics and Technical Physics **42**, 851 (2001)
[9] V.Ì. Paskonov, V.I. Polezhayev, L.À. Chudov, Numerical simulation of heat and mass transfer processes (1984)
[10] G.V. Kuznetsov, M.A. Sheremet, J. Thermophysics and Aeromechanics **16**, 119 (2009)
[11] G.V. Kuznetsov, M.A. Sheremet, J. Russian Microelectronics **37**, 131 (2008)
[12] G.V. Kuznetsov, P.A. Strizhak, J. Engineering Thermophysics **18**, 72 (2009)
[13] G.V. Kuznetsov, P.A. Strizhak, J. Engineering Thermophysics **18**, 162 (2009)
[14] O.V. Vysokomornaya, G.V. Kuznetsov, P.A. Strizhak, J. Russian Physical Chemistry **5**, 668 (2011)
[15] G.V. Kuznetsov, P.A. Strizhak, J. Engineering Thermophysics **17**, 244 (2008)
[16] E.L. Tarunin, Computational experiment in the problems on free convection (1990)
[17] A.A. Samarskiy, P.N. Vabischevitch, Computational heat transfer (2003)